Submitted: 07 April, 2025 Accepted: 08 May, 2025 Published: 08 July, 2025 DOI:10.22514/sv.2025.102

Open Access
Signa Vitae

ORIGINAL RESEARCH

Sodium aesculin alleviates inflammation and pyroptosis in cardiomyocytes induced by methyl parathion *in vivo* and *in vitro* AOPP model

Zhan Su[1], Dingming Liu[2], Hongxiang Yang[2], Junjie Wen[2,*]

[1]HIFU Medical Center, Guang'an People's Hospital, 638000 Guang'an, Sichuan, China
[2]Department of Cardiovascular, Guang'an People's Hospital, 638000 Guang'an, Sichuan, China

***Correspondence**
Wenjunjie_666@163.com
(Junjie Wen)

Abstract

Background: Acute organophosphorus pesticide poisoning (AOPP) is a prevalent cause of drug-related poisoning in hospital emergency departments, yet the mechanisms underlying myocardial damage remain poorly understood. Sodium aesculin, the active compound found in Aesculin, has demonstrated promising anti-inflammatory and antioxidant properties. However, its effects on myocardial injury induced by AOPP have not been thoroughly investigated. This study aims to explore the potential protective effects of sodium aesculin (SA) on methyl parathion (MP)-induced cardiomyocyte injury. **Methods**: MP-induced cardiomyocytes were utilized as an experimental cell model. Cell viability was assessed using Cell Counting Kit-8 (CCK-8) assay, which provided insights into the compound's effects on cellular proliferation. Quantitative Polymerase Chain Reaction (qPCR) was employed to evaluate the impact of Sodium aesculin on inflammatory responses and pyroptotic cell death within both cellular and rat models. Immunoblot assays were further conducted to confirm the mechanism. **Results**: Using CCK-8, qPCR and immunoblot assays in H9C2 cells and rats, we observed that SA increased MP-impaired cell viability ($p < 0.01$). A dosage of 1.5 mg/kg SA reduced cardiac inflammation ($p < 0.001$) and pyroptosis ($p < 0.001$) compared to MP controls. Mechanistically, sodium aesculin inhibits MP-induced Nuclear Factor Kappa-Light-Chain-Enhancer of Activated B Cells (NF-κB) activation ($p < 0.001$). **Conclusions**: Sodium aesculin (SA) alleviates inflammation and pyroptosis in MP-induced cardiomyocytes, suggesting its potential as a therapeutic agent for AOPP-related myocardial injury.

Keywords

Acute organophosphorus pesticide poisoning (AOPP); Cardiomyocyte; Inflammation; Pyroptosis; NF-κB

1. Introduction

Organophosphorus pesticides are among the most widely used insecticides, particularly in rural or underdeveloped regions of developing countries [1]. Acute organophosphorus pesticide poisoning (AOPP) is frequently encountered in hospital emergency departments, and the pathogenesis of AOPP has been thoroughly examined [2]. These pesticides irreversibly bind to the active site of acetylcholinesterase, resulting in the phosphorylation of the enzyme. This process leads to the accumulation of acetylcholine and inhibits the activity of acetylcholinesterase [3]. The clinical manifestations of organophosphorus pesticide exposure on myocardial injury vary from patient to patient, including arrhythmia, heart failure, cardiogenic shock, and sudden death [4]. Additionally, organophosphorus induces oxidative stress, inflammation, and apoptosis by producing free radicals [5]. To better understand the myocardial damage caused by AOPP, further research into its mechanisms and the development of effective antidotes is essential [3].

The activation of cytokine receptors, pattern recognition receptors, or T and B cell receptors stimulates the IκB kinase (IKK) complex, resulting in the phosphorylation and subsequent degradation of IκBα [6]. The NF-κB signal transduction pathway is activated in response to parathion exposure [6]. Exposure to parathion activates the NF-κB signal transduction pathway. This activation leads to an upregulation in the transcription of inflammation-related components, such as Nucleotide-binding Leucine-rich Repeat Pyrin domain-containing protein 3 (NLRP3), Proform of Interleukin-1β (pro-IL-1β) and pro-IL-18 [7]. Subsequently, the inflammasome adaptor protein (apoptosis-associated speck-like protein containing a caspase recruitment domain) ASC is recruited to NLRP3, which interacts with caspase-1, facilitating its activation. Once activated, caspase-1 catalyzes the maturation

of the pro-inflammatory cytokines IL-1β and IL-18, helping to alleviate myocardial pyrosis and inflammation via the NF-κB/NLRP3 pathway [8, 9].

Hippocastanaceae is a plant found worldwide. SA, the primary active compound in Aesculin, a coumarin glycoside organic compound, has demonstrated a protective effect against liver damage caused by methyl parathion poisoning owing to its anti-inflammatory and antioxidant properties [10]. Previous research has also indicated that SA can mitigate myocardial damage resulting from MP poisoning, thereby alleviating oxidative stress, and reducing apoptosis in cardiomyocytes [3].

This study hypothesizes that SA can protect against myocardial injury induced by MP poisoning. While previous studies have examined organophosphorus-induced oxidative stress, the role of pyroptosis in AOPP-related cardiac injury remains unexplored. Emerging evidence suggests that MP induces cardiomyocyte pyroptosis through NLRP3 inflammasome activation, leading to irreversible contractile impairment, a significant contributor to AOPP-related cardiac failure. Our study is the first to demonstrate that SA specifically targets the NF-κB-pyroptosis axis, presenting a novel therapeutic approach for AOPP-induced myocardial damage.

2. Materials and methods

2.1 Cell culture and treatment

Cardiomyocyte H9C2 cells were sourced from the Chinese Academy of Sciences. The cells were cultured in Dulbecco's Modified Eagle Medium (DMEM, 12800017, Gibco, Grand Island, NY, USA) supplemented with 10% fetal bovine serum (FBS, 10099141C, Gibco, Grand Island, NY, USA) and 1% penicillin-streptomycin (P4333, Sigma, St. Louis, MO, USA) in a humidified incubator at 37 °C with 5% CO_2. The H9C2 rat cardiomyocyte cell line was obtained from the Cell Bank of Chinese Academy of Sciences (Shanghai, China) and authenticated by short tandem repeat (STR) profiling. Cells were used within 15 passages and maintained under standard culture conditions (DMEM + 10% FBS at 37 °C, 5% CO_2). For the construction of the MP model, the cells were cultured in DMEM, treated with MP (20 mM, M5293, bought from Sigma, St. Louis, MO, USA), and maintained at 37 °C for 24 h. Timepoints for sample collection were standardized at 24 h post-treatment.

2.2 Rat model

Male Sprague-Dawley rats (8 weeks old, 250–280 g, n = 6 in each group) were purchased from Vital River (Beijing, China) and housed in standard cages under a 12-hour light/dark cycle at a temperature of 22–24 °C and humidity of 50–60%. The rats had unrestricted access to food and water and libitum throughout the experiment. Following the experimental period, the rats were humanely euthanized by inhalation of isoflurane, followed by cervical dislocation to ensure a rapid and painless procedure. Heart tissues were immediately harvested, rinsed with ice-cold phosphate-buffered saline (PBS), and stored at −80 °C for subsequent analysis. For histological examination, tissues were fixed in 10% formalin and processed for paraffin embedding. For the construction of an AOPP model, an intraperitoneal injection of 10 mg/kg of MP was administered to the rats, followed by the administration of SA (0.5, 1 and 1.5 mg/kg, S5922, procured from Sigma, St. Louis, MO, USA) through intraperitoneal injection. The doses of SA and MP were chosen according to the previous study [4]. The rats were categorized into the following groups: control, MP (10 mg/kg), SA (0.5 mg/kg) + MP (10 mg/kg), SA (1 mg/kg) + MP (10 mg/kg), as well as SA (1.5 mg/kg) + MP (10 mg/kg), groups. Ethical approval was obtained from the Ethics Committee of Guang'an People's Hospital (Approval no. 2023XM0019).

2.3 Cell viability assay

H9C2 cells were seeded into 96-well plates at a density of 1000 cells per well and incubated for 24 h to allow attachment. The doses of SA and MP were selected based on a previous study [4]. The cells were then treated with sodium aesculin (SA) or methyl parathion (MP) as specified, and incubated with 10 μL of CCK-8 reagent (CK04, Dojindo, Kumamoto, Japan) for 4 hours at 37 °C. The absorbance at 450 nm (OD450) was measured using a microplate reader (210125, BioTek, Winooski, VT, USA) to evaluate cell viability, with the OD450 value indicative of the number of viable cells.

2.4 Immunoblotting

Radio Immuno Precipitation Assay buffer (RIPA) lysis buffer was added to the cells or tissues and incubated on ice for 30 minutes to lyse the samples and extract the proteins fully. The protein concentration was then quantified using the Beyotime Bicinchoninic Acid assay (BCA) protein assay kit (P0011, Beijing, China) according to the manufacturer's instructions. Sodium Dodecyl Sulfate-PolyAcrylamide Gel Electrophoresis (SDS-PAGE) separated equal amounts of protein, which were subsequently transferred onto Polyvinylidene Difluoride (PVDF) membranes using a semi-dry transfer method. The proteins were blocked with 5% milk for 1 h. Primary antibodies including NLRP3 (1:1000, ab263899, Abcam, Cambridge, UK), caspase 1 (1:1000, ab207802), IL-1β (1:500, ab216995), IL-18 (1:1000, ab243091), p65 (1:500, ab32536), p-p65 (S536, 1:500, ab76302, Abcam, Cambridge, UK), IκBα (1:1000, 9242#, Cell signaling, Danvers, MA, USA), p-IκBα (1:1000, 2859#, Cell signaling, Danvers, MA, USA), GAPDH (Glyceraldehyde-3-Phosphate Dehydrohydrogenase) (1:3000; ab8245, Abcam, Cambridge, UK), and secondary antibodies were incubated for 1 h and photographed after chemiluminescence. Pyroptosis quantification was performed by measuring the expression of caspase-1 and NLRP3, with all protein bands normalized to GAPDH as the internal control.

2.5 qPCR assay

Total RNA was extracted from cells utilizing TRIzol reagent (15596026, Thermo Fisher, Rockford, IL, USA) following the manufacturer's instructions. The quality and concentration of the RNA were assessed using a NanoDrop spectrophotometer. One microgram of RNA was reverse transcribed into cDNA using Moloney Murine Leukemia Virus reverse transcriptase (M-MLV) reverse transcriptase (M1705 Promega, Madison,

WI, USA). The cDNA was then employed for quantitative PCR (qPCR) with SYBR Green PCR Master Mix (4309155, Thermo Fisher, Waltham, MA, USA) and specific primers for target genes. qPCR was performed on a QuantStudio 3 system (A43179, Thermo Fisher, Waltham, MA, USA), and gene expression was normalized to GAPDH using the $2^{-\Delta\Delta Ct}$ method. The cDNA was amplified using the following primers: Tumor Necrosis Factor-α (or Tumor Necrosis Factor-alpha (TNF-α): 5′-CTCCGGGCTCAGAATTTCC-3′, 5′-CGCAATCCAGGCCACTACTT-3′; IL-1β: 5′-ATAGCG TGACATTAAGAG-3′, 5′-GTGACGATAGTGATGACCT-3′; IL-6: 5′-CCACCAGGAACGAAAGTCAAC-3′, 5′-GGCAG TGGCTGTCAACAACA-3′; NLRP3: 5′-TTGAAGAGGAG TGGATAGGT-3′, 5′-GGTGTAGCGTCTGTTGAG-3′; caspase-1: 5′-TGGATTGCTGGATGAACTT-3′, 5′-CTGATG GACCTGACTGAAG-3′; IL-18: 5′-TGGAATCAGACCACT TTGGC-3′, 5′-GTCTGGTCTGGGATTCGTTG-3′; GAPDH: 5′-ACGGCAAGTTCAACGGCACAG-3′, 5′-GAC GCCAGTAGACTCCACGACA-3′.

2.6 ELISA assay

To further validate the inflammatory responses, we performed an enzyme-linked immunosorbent assay (ELISA) to measure the protein levels of TNF-α, IL-1β and IL-6 in the cell culture supernatants. The ELISA kits (PI301, PI303, and PI326, respectively, Biyotime, Beijing, China) were used following the manufacturer's protocols. Absorbance was measured at 450 nm using a microplate reader (BioTek, USA). All assays were conducted in triplicate.

2.7 Statistical analysis

All comparisons between multiple groups were conducted using one-way Analysis of Variance (ANOVA) (for single-factor experiments) or two-way ANOVA (for time/dose interactions), accompanied by Tukey's *post-hoc* test, as specified in the figure legends. Data normality was confirmed via Shapiro-Wilk tests ($p > 0.05$ for all datasets), and variance homogeneity was verified using Levene's test prior to ANOVA application.

3. Results

3.1 Sodium aesculin promotes MP-induced myocardial cell viability

To elucidate the effects of SA on AOPP-induced myocardial injury, a model was constructed using H9C2 cells. These cells were utilized to create an *in vitro* model through MP. CCK-8 assays revealed that SA had modest effects on the viability of H9C2 cells at lower concentrations (10, 30 and 50 μM). In comparison, higher concentrations (80, 100 μM) of SA significantly suppressed the viability of H9C2 cells (Fig. 1A). Consequently, the lower concentrations of SA were selected for further *in vitro* assays. Additionally, while MP treatment reduced the viability of H9C2 cells, SA at concentrations of 10, 30 and 50 μM effectively reversed the decline in cell viability induced by MP treatment (Fig. 1B). Therefore, SA promotes MP-treated H9C2 cell viability.

3.2 Sodium aesculin inhibits MP-induced cardiomyocyte inflammation

The effects of SA on the inflammation of MP-induced H9C2 cells were assessed. ELISA assays revealed the mRNA levels of inflammatory factors, including TNF-α, IL-6 and IL-1β. MP stimulated the increase of mRNA levels of these factors in H9C2 cells (Fig. 2A). However, SA treatment mitigated the increase in the mRNA levels of these inflammatory factors induced by MP treatment in H9C2 cells (Fig. 2A). Similarly, SA treatment alleviated the increase in the secretion levels of these inflammatory factors induced by MP treatment in H9C2 cells, which was confirmed by ELISA (Fig. 2B). Collectively, these findings indicate that SA treatment mitigates MP-induced inflammation in H9C2 cells.

3.3 Sodium aesculin inhibits MP-induced myocyte pyroptosis

To investigate whether SA affects pyroptosis in H9C2 cells after MP treatment, we evaluated the expression of key pyroptosis markers. We aimed to determine the impact of SA on the pyroptosis of H9C2 cells after MP exposure. The results from qPCR assays indicated elevated mRNA levels of pyroptosis markers, including NLRP3, caspase-1, and high expression of inflammatory factors such as IL-18 and IL-1β in MP-induced H9C2 cells (Fig. 3A). Notably, SA treatment suppressed the mRNA levels of these factors after MP treatment in H9C2 cells (Fig. 3A). Similarly, immunoblot assays demonstrated that SA treatment decreased the protein levels of these markers in MP-induced H9C2 cells (Fig. 3B). Therefore, SA inhibits MP-induced pyroptosis of H9C2 cells.

3.4 Sodium aesculin inhibits myocardial inflammation and pyroptosis in MP-induced rats

To further validate the previous findings, we examined the effects of SA in a rat model of MP-induced myocardial injury. qPCR assays showed elevated mRNA levels of inflammatory markers including TNF-α, IL-18 and IL-1β, in heart tissues of rats treated with MP (Fig. 4A). In contrast, treatment with SA significantly reduced the mRNA levels of these factors in heart tissues of rats treated with MP (Fig. 4A). Additionally, immunoblot assays demonstrated increased expression of NLRP3, caspase-1, IL-18 and IL-1β in heart tissues from MP-treated rats. In contrast, SA treatment decreased the expression of these proteins (Fig. 4B). Therefore, SA inhibits myocardial inflammation and pyroptosis in MP-induced rats.

3.5 Sodium aesculin inhibits MP-induced NF-κB activation *in vivo* and *in vitro*

To investigate the underlying mechanism by which SA alleviates MP-induced injury in H9C2 cells and rat heart tissues, we investigated the effects of SA on the activation of the NF-κB signaling pathway. The mechanism underlying SA relieving MP-induced injury of H9C2 cells and heart tissues of rats was subsequently determined. Treatment with MP resulted in the phosphorylation of p65 and IκBα while reducing the expression of IκBα in H9C2 cells (Fig. 5A). However, SA treatment

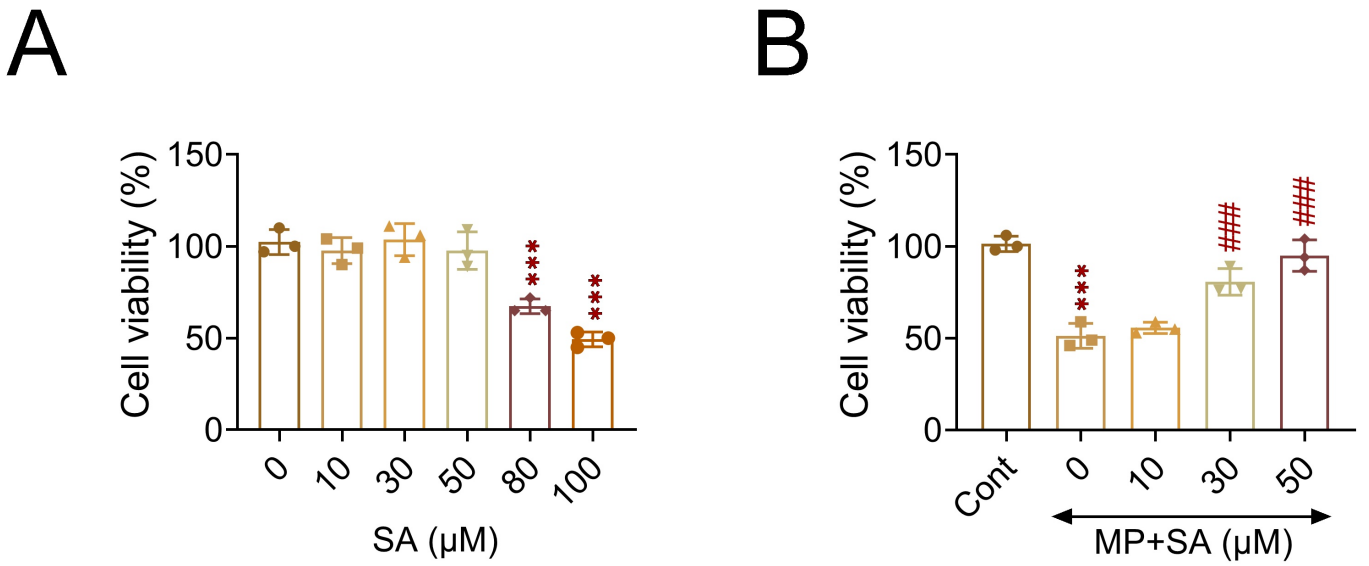

FIGURE 1. Sodium aesculin promotes MP-induced myocardial cell viability. (A) CCK-8 assays showed the effects of SA on the growth of H9C2 cells at the concentrations of 10, 30, 50, 80 and 100 μM for 24 h. The OD450 value was measured. ***$p < 0.001$, SA *vs*. control. (B) CCK-8 assay showed the effects of SA on the growth of H9C2 cells at the concentrations of 10, 30 and 50 μM upon treating MP for 24 h. The OD450 value was measured. ***$p < 0.001$, SA *vs*. control. ***$p < 0.001$, MP *vs*. control, $^{\#\#\#}p < 0.001$, MP + SA *vs*. MP. SA, Sodium aesculin; MP, methyl parathion; Cont: control.

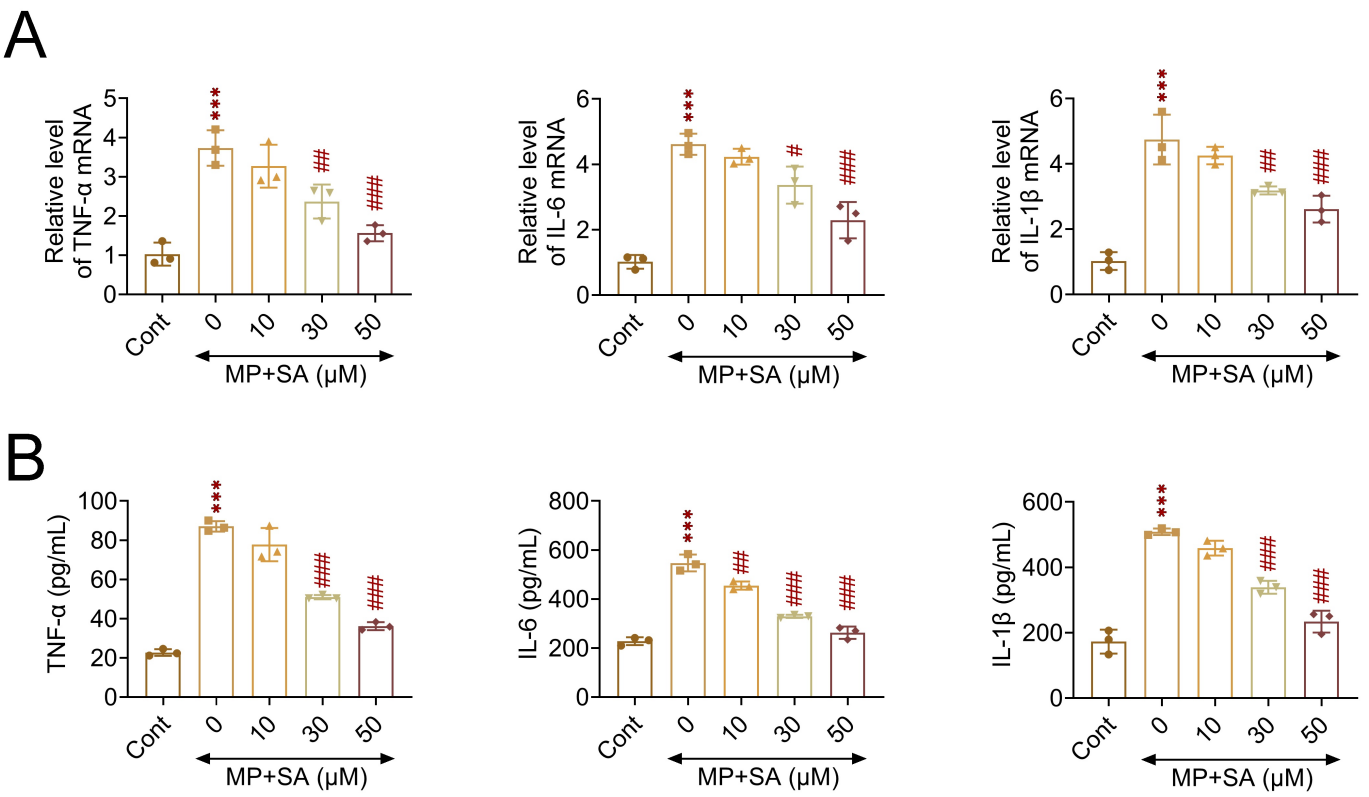

FIGURE 2. Sodium aesculin inhibits MP-induced cardiomyocyte inflammation. (A) qPCR assays showed the mRNA levels of TNF-α, IL-6 and IL-1β in H9C2 cells upon SA treatment at the concentrations of 10, 30 and 50 μM, following the treatment of MP for 24 h. (B) ELISA assays showed the secretion levels of TNF-α, IL-6 and IL-1β in H9C2 cells upon SA treatment at the concentrations of 10, 30 and 50 μM, following the treatment of MP for 24 h. ***$p < 0.001$, SA *vs*. control. ***$p < 0.001$, MP *vs*. control, $^{\#}p < 0.05$, $^{\#\#}p < 0.01$, $^{\#\#\#}p < 0.001$, MP + SA *vs*. MP. SA, Sodium aesculin; MP, methyl parathion; TNF, Tumor Necrosis Factor; IL, Interleukin; Cont, control.

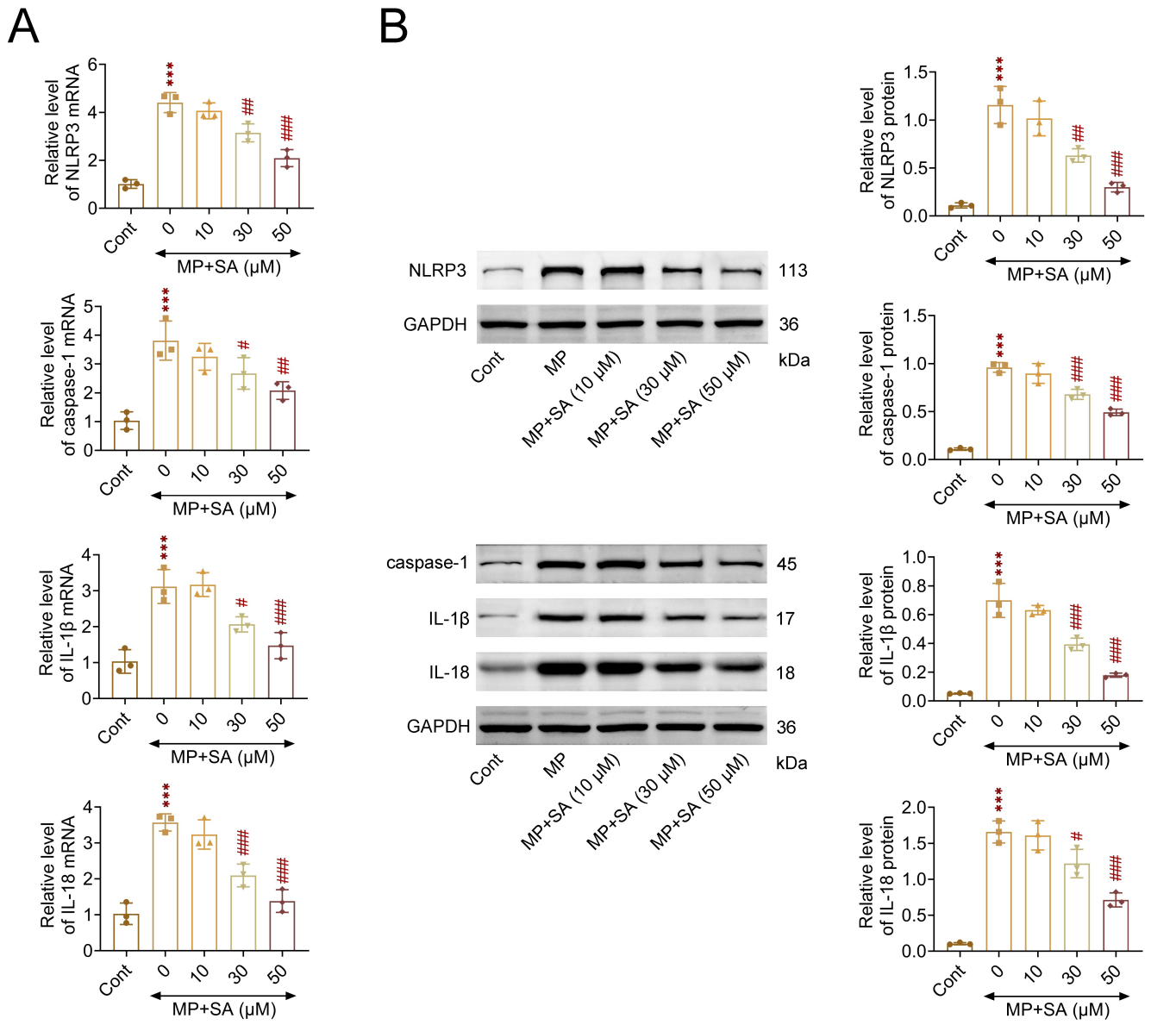

FIGURE 3. Sodium aesculin inhibits MP-induced myocyte pyroptosis. (A) qPCR assays showed the mRNA levels of NLRP3, caspase-1, IL-1β and IL-18 in H9C2 cells upon SA treatment at the concentration of 10, 30 and 50 μM upon the treatment of MP for 24 h. (B) Immunoblot assays showed the expression levels of NLRP3, caspase-1, IL-1β and IL-18 in H9C2 cells upon SA treatment at the concentration of 10, 30 and 50 μM upon the treatment of MP for 24 h. ***$p < 0.001$, SA *vs.* control. ***$p < 0.001$, MP *vs.* control, $^{\#}p < 0.05$, $^{\#\#}p < 0.01$, $^{\#\#\#}p < 0.001$, MP + SA *vs.* MP. SA, Sodium aesculin; MP, methyl parathion; NLRP3, Nucleotide-binding oligomerization Leucine-rich Repeat and Pyrin domain-containing protein 3; IL, Interleukin; Cont, control; GAPDH, Glyceraldehyde-3-Phosphate Dehydrohydrogenase.

effectively reversed the decrease in IκBα expression. The promotion of p65 and IκBα phosphorylation in H9C2 cells induced by MP treatment (Fig. 5A). Similarly, immunoblot assays confirmed that SA treatment countered the effects of MP on IκBα expression and the phosphorylation of p65 and IκBα in rat heart tissues, aligning with our previous results (Fig. 5B). These data suggest that SA inhibits MP-induced NF-κB activation *in vivo* and *in vitro*.

4. Discussion

Acute organophosphorus pesticide poisoning (AOPP) results from rapid exposure to organophosphates, leading to toxicity through acetylcholinesterase (AChE) inhibition [11]. This inhibition causes an accumulation of acetylcholine in the tissues, disrupting cholinergic receptor activity and resulting in organ dysfunction [12]. The fatality rate associated with AOPP varies based on the type, dose, and timing of the exposure, with a high mortality rate observed in severely poisoned patients [3]. Recent advancements in the treatment of AOPP, ranging from cholinesterase inhibitors to novel therapeutic approaches, have significantly improved patient outcomes [13]. Our findings indicate that sodium aescinate (SA) provides cardioprotection in MP-induced injury primarily through the dual inhibition of NF-κB-mediated inflammation and NLRP3-dependent pyroptosis.

AOPP induces arrhythmias through cholinesterase inhibi-

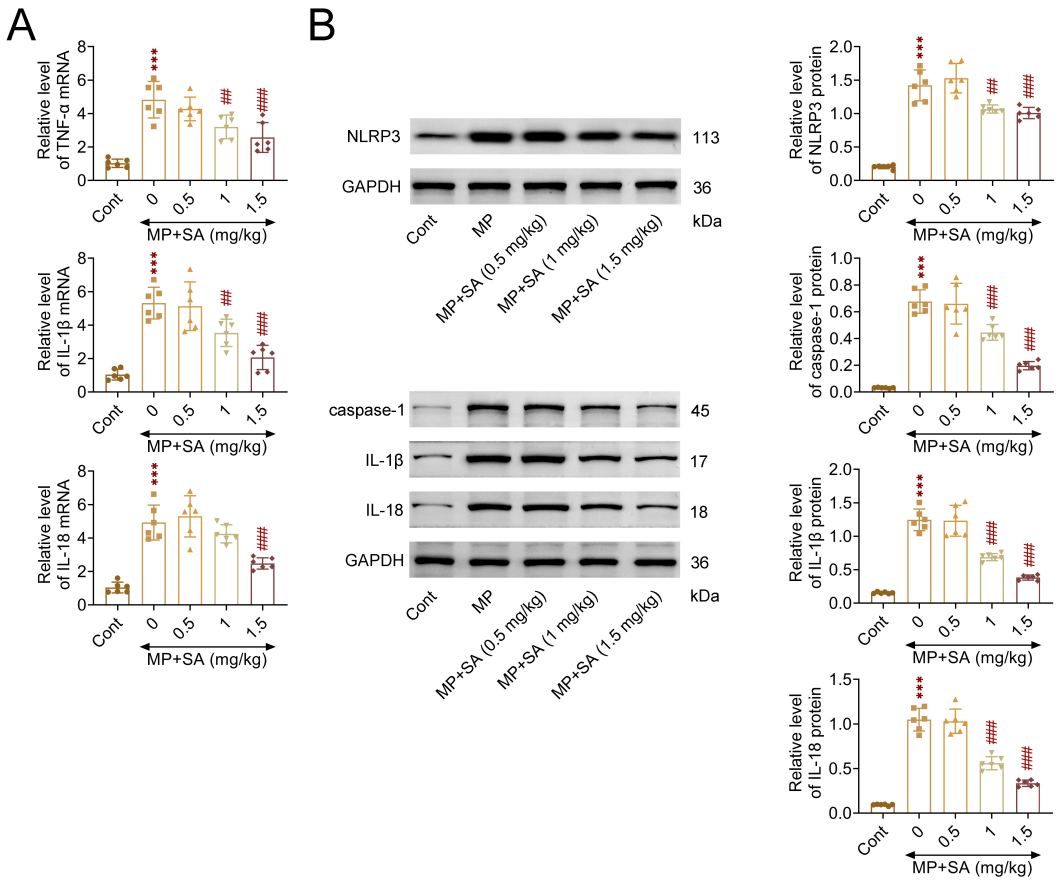

FIGURE 4. Sodium aesculin inhibits myocardial inflammation and pyroptosis in MP-induced rats. (A) qPCR assays showed the mRNA levels of TNF-α, IL-1β and IL-18 in heart tissues from rats upon treatment of SA at the concentration of 0.5, 1, 1.5 mg/kg upon the treatment of MP for 24 h. (B) Immunoblot assays showed the expression levels of NLRP3, caspase-1, IL-1β and IL-18 in from rats upon treatment of SA at the concentration of 0.5, 1, 1.5 mg/kg upon the treatment of MP for 24 h. ***$p < 0.001$, SA *vs.* control. ***$p < 0.001$, MP *vs.* control, $^{\#\#}p < 0.01$, $^{\#\#\#}p < 0.001$, MP + SA *vs.* MP. SA, Sodium aesculin; MP, methyl parathion; NLRP3, Nucleotide-binding oligomerization Leucine-rich Repeat and Pyrin domain-containing protein 3; IL, Interleukin; Cont, Control; GAPDH, Glyceraldehyde-3-Phosphate Dehydrohydrogenase; TNF, Tumor Necrosis Factor.

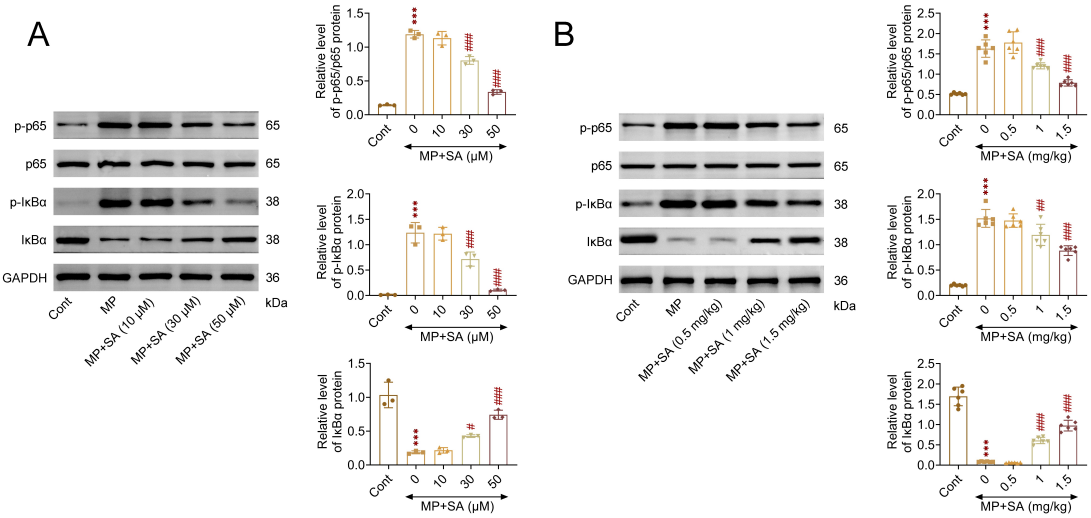

FIGURE 5. Sodium aesculin inhibits MP-induced NF-κB activation *in vivo* and *in vitro*. (A) Immunoblot assays showed the expression and phosphorylation levels of p65 and IκBα in H9C2 cells upon SA treatment at the concentration of 10, 30 and 50 μM upon the treatment of MP for 24 h. (B) Immunoblot assays showed the expression and phosphorylation levels of p65 and IκBα in from rats upon treatment of SA at the concentration of 0.5, 1, 1.5 mg/kg upon the treatment of MP for 24 h. ***$p <$ 0.001, SA or MP *vs.* control. $^{\#}p < 0.05$, $^{\#\#}p < 0.01$, $^{\#\#\#}p < 0.001$, MP + SA *vs.* MP. SA, Sodium aesculin; MP, methyl parathion; IκBα, Inhibitor of κBα; GAPDH, Glyceraldehyde-3-Phosphate Dehydrohydrogenase; Cont, control.

tion (causing acetylcholine accumulation) or direct cardiomyocyte toxicity [2]. The cardiac damage resulting from AOPP compromises myocardial contractility due to ischemic injury, which may progress to toxic myocarditis. Although SA exhibits multi-organ protective effects against AOPP, its cardioprotective mechanisms are not yet fully understood. Our findings show that SA significantly alleviates myocardial injury induced by methyl parathion (MP), providing new insights into its potential therapeutic effects on AOPP-related heart damage.

In cardiomyocytes, pyroptosis contributes to the pathogenesis of myocardial infarction, cardiac ischemia-reperfusion injury, diabetic cardiomyopathy, and other diseases [7, 14]. Pyroptosis plays a critical role in myocardial injury stemming from various diseases and can occur via classical, non-classical, and Caspase 3-mediated pathways [15]. Notably, SA inhibits myocardial inflammation and pyroptosis in MP-induced rats. The exact mechanism by which this occurs requires further investigation.

Dysregulation of NF-κB has been linked to a variety of human diseases such as cancer, inflammatory and autoimmune diseases, viral infections, septic shock, and abnormal development of the immune system [16]. Pyroptosis is a form of inflammatory cell death triggered by the NF-κB signaling pathway [17]. The NF-κB signaling pathway plays a crucial role in numerous physiological and pathological processes, such as immune response, inflammation, cell survival, and proliferation [18–20]. In this study, SA inhibits MP-induced NF-κB activation, as evidenced by examining p65 and IκBα phosphorylation levels. These results support the NF-κB pathway as a promising target for AOPP treatment. Our study specifically investigates the myocardial protective effects of SA and its underlying mechanisms, with a particular focus on the NF-κB signaling pathway and pyroptosis. The novelty of our research lies in the detailed exploration of these mechanisms in the heart, a topic that has not been thoroughly addressed in previous research.

Our study illustrates that SA significantly reduces inflammation and pyroptosis in cardiomyocyte injury induced by MP. By targeting key inflammatory pathways and mechanisms of cell death, sodium aesculin may act as a promising therapeutic agent in mitigating myocardial damage caused by organophosphate toxicity. These findings offer valuable insights into the molecular mechanisms of MP-induced cardiac injury and suggest that targeting inflammation and pyroptosis could be an effective strategy for therapeutic intervention.

However, this study has limitations, including the absence of *in vivo* long-term follow-up to evaluate the lasting effects of sodium aesculin on cardiac function and recovery. Furthermore, the precise molecular targets of sodium aesculin in modulating pyroptosis and inflammation warrant further investigation to comprehend its therapeutic potential in AOPP fully.

The preferential suppression of IL-1β and IL-18 by SA, as opposed to other cytokines such as TNF-α, indicates its targeted inhibition of the NLRP3 inflammasome, which is the canonical pathway for processing pro-IL-1β and IL-18. While our study highlights the acute cardioprotective effects of SA, the lack of histological scoring and long-term functional monitoring necessitates caution when extrapolating the results to chronic recovery scenarios. Furthermore, although NF-κB inhibition seems to play a central role, the potential off-target effects of SA on related pathways remain to be elucidated. Future studies should incorporate longitudinal echocardiography to track functional recovery, single-cell RNA sequencing to identify SA-responsive cardiomyocyte subpopulations, and comparative studies with standard AOPP therapies to assess clinical translatability. SA could complement existing treatment regimens for severe AOPP cases involving myocardial damage, though clinical synergy studies are warranted.

5. Conclusions

SA reduces myocardial inflammation and pyroptosis in MP-induced rats by inhibiting NF-κB activation *in vivo* and *in vitro*. Therefore, SA could serve as a promising drug for AOPP treatment.

AVAILABILITY OF DATA AND MATERIALS

The authors declare that all data supporting the findings of this study are available within the paper and any raw data can be obtained from the corresponding author upon request.

AUTHOR CONTRIBUTIONS

ZS, DML, HXY and JJW—designed the study and carried them out; supervised the data collection. ZS, DML and JJW—analyzed and interpreted the data. ZS and JJW—prepared the manuscript for publication and reviewed the draft of the manuscript. All authors have read and approved the manuscript.

ETHICS APPROVAL AND CONSENT TO PARTICIPATE

Ethical approval was obtained from the Ethics Committee of Guang'an People's Hospital (Approval no. 2023XM0019).

ACKNOWLEDGMENT

Not applicable.

FUNDING

This work was supported by Sichuan government Transfer payment project (Grant No. 2021ZYZFSY01), Scientific and technological innovation guiding plan project of Guang'an (Grant No. 2021zdxjh13) and Guang'an People's Hospital High Quality Development Fund Project (Grant No. 21FZ009).

CONFLICT OF INTEREST

The authors declare no conflict of interest.

REFERENCES

[1] Wen SH, Zhang H, Yu S, Ma J, Zhu JJ, Zhou Y. Complementary homogeneous electrochemical and photothermal dual-modal sensor for highly sensitive detection of organophosphorus pesticides via stimuli-responsive COF/methylene blue@MnO_2 composite. Analytical Chemistry. 2023; 95: 14914–14924.

[2] Kaur S, Chowdhary S, Kumar D, Bhattacharyya R, Banerjee D. Organophosphorus and carbamate pesticides: molecular toxicology and laboratory testing. Clinica Chimica Acta. 2023; 551: 117584.

[3] Liu S, Lu J, Li Z. Water quality criteria derivation and ecological risk assessment for organophosphorus pesticides. Chemosphere. 2024; 348: 140726.

[4] Porey C, Jha M, Bhoi SK, Samal P, Naik S. A study of organophosphorus induced delayed myelopathy: uncommon sequelae of a common poisoning. Annals of Indian Academy of Neurology. 2023; 26: 469–474.

[5] Islam A, Chowdhury D, Palit PK, Sohel M, Mozibullah M, Islam MJ, *et al*. Serum creatinine phosphokinase: a potential prognostic marker in assessing clinical severity with organophosphorus poisoning. Journal of Clinical Laboratory Analysis. 2023; 37: e24980.

[6] Shin C, Ito Y, Ichikawa S, Tokunaga M, Sakata-Sogawa K, Tanaka T. MKRN2 is a novel ubiquitin E3 ligase for the p65 subunit of NF-κB and negatively regulates inflammatory responses. Scientific Reports. 2017; 7: 46097.

[7] Zhang X, Chen W, Liu W, Li D, Shen W. CITED2 alleviates lipopolysaccharide-induced inflammation and pyroptosis in-human lung fibroblast by inhibition of NF-κB pathway. Allergologia et Immunopathologia. 2022; 50: 64–70.

[8] Wang Z, Zhu X, Huang ZZ, Ren KD, Ran J, Yang Y. Histone deacetylase 6 (HDAC6) in ciliopathies: emerging insights and therapeutic implications. Advanced Science. 2025; 12: e2412921.

[9] Xu J, Liu J, Li Q, Mi Y, Zhou D, Wang J, *et al*. Loureirin C ameliorates ischemia and reperfusion injury in rats by inhibiting the activation of the TLR4/NF-κB pathway and promoting TLR4 degradation. Phytotherapy Research. 2022; 36: 4527–4541.

[10] DePamphilis CW, Wyatt R. Electrophoretic confirmation of interspecific hybridization in aesculus (Hippocastanaceae) and the genetic structure of a broad hybrid zone. Evolution. 1990; 44: 1295–1317.

[11] Gong C, Chen B, Xing Y, Zhao H. Metal-pyrimidine nanocubes immobilized enzymes with pH-switchable multienzyme-like activity for broad-pH-responsive sensing assay for organophosphorus pesticides. Journal of Hazardous Materials. 2024; 463: 132849.

[12] Gull M, Feng T, Smith B, Calcul L, Pasek MA. Prebiotic syntheses of organophosphorus compounds from reduced source of phosphorus in non-aqueous solvents. Life. 2023; 13: 2134.

[13] Wang W, Xiong Z, Zeng X. Polygonum cuspidatum glycoside mitigated LPS-induced human endometrial stromal cell inflammation by regulating NF-κB/Nrf2 signaling pathway-related proteins. Tropical Journal of Pharmaceutical Research. 2022; 21: 495–499.

[14] Pan H, Lin Y, Dou J, Fu Z, Yao Y, Ye S, *et al*. Wedelolactone facilitates Ser/Thr phosphorylation of NLRP3 dependent on PKA signalling to block inflammasome activation and pyroptosis. Cell Proliferation. 2020; 53: e12868.

[15] Wei Y, Yang L, Pandeya A, Cui J, Zhang Y, Li Z. Pyroptosis-induced inflammation and tissue damage. Journal of Molecular Biology. 2022; 434: 167301.

[16] Liu Z, Chen B, Chang J, Feng L, Zhao X. Melatonin regulates trophoblast pyroptosis, invasion and migration in preeclampsia by inhibiting HtrA1 transcription through the microRNA-520c-3p/SETD7 axis. American Journal of Reproductive Immunology. 2022; 87: e13523.

[17] Bai J, Deng S, Zhang X, Dai Z, Ji Y, Zeng S, *et al*. Cinnamaldehyde alleviates zearalenone-induced LS174T cell apoptosis, barrier dysfunction and mucin reduction through JNK/NF-κB signaling pathway. Ecotoxicology and Environmental Safety. 2023; 263: 115276.

[18] Zhou Q, Cheng C, Wei Y, Yang J, Zhou W, Song Q, *et al*. USP15 potentiates NF-κB activation by differentially stabilizing TAB2 and TAB3. The FEBS Journal. 2020; 287: 3165–3183.

[19] Yu L, Tian D, Su Z, Zhang L, Jie L, Guo S, *et al*. Mechanical stress overload promotes NF-κB/NLRP3-mediated osteoarthritis synovitis and fibrosis through Piezo1. Cellular Signalling. 2025; 132: 111786.

[20] Ma Y, Wu Z, Tu Y, Liu C, Guo J, Xu Y, *et al*. Hypoxia-inducible factor-1α involves in regulating anti-lipopolysaccharide factors expression via NF-κB under hypoxia stress in Chinese mitten crab (Eriocheir sinensis). Fish and Shellfish Immunology. 2025; 162: 110328.

How to cite this article: Zhan Su, Dingming Liu, Hongxiang Yang, Junjie Wen. Sodium aesculin alleviates inflammation and pyroptosis in cardiomyocytes induced by methyl parathion *in vivo* and *in vitro* AOPP model. Signa Vitae. 2025; 21(7): 103-110. doi: 10.22514/sv.2025.102.